Journal of Applied Polymer Science

Preparation and Characterization of Plasticized Starch/Halloysite Porous Nanocomposites Possibly Suitable for Biomedical Applications

Helene Schmitt, Nicolas Creton, Kalappa Prashantha, Jeremie Soulestin, Marie-France Lacrampe, Patricia Krawczak

Mines Douai, Department of Polymers and Composites Technology & Mechanical Engineering, 941 rue Charles Bourseul, CS 10838, F-59508 Douai Cedex France

Correspondence to: K. Prashantha (E-mail: kalappa.prashantha@mines-douai.fr)

ABSTRACT: Novel porous bionanocomposites based on halloysite nanotubes as nanofillers and plasticized starch as polymeric matrix were successfully prepared by melt-extrusion. Foaming was obtained by adding water as natural blowing agent, and by increasing the die temperature. Both the expansion ratio and the porosity increase with increasing die temperature. Addition of high water content allows reducing the foaming temperature. Moreover, the introduction of halloysite has double benefits: these fillers act both as a nucleating agent increasing the porosity and as a barrier agent increasing the proportion of small cells. Foams based on plasticized starch with a blend of glycerol and sorbitol loaded with 6 wt % of halloysite, extruded at 117°C, present the cellular structure and the mechanical properties required for scaffold applications. © 2014 Wiley Periodicals, Inc. J. Appl. Polym. Sci. **2015**, *132*, 41341.

KEYWORDS: biomaterials; extrusion; foams

Received 18 December 2013; accepted 27 July 2014
DOI: 10.1002/app.41341

INTRODUCTION

In recent years, the development of porous materials increases especially in biomedical domain such as scaffolds in tissue engineering for bones and cartilages or as drug delivery systems. According to the application, the material requirements can greatly vary. For example, for scaffolds, a compromise must be found between porosity and mechanical strength.[1]

In the case of biomaterials loaded with therapeutic agents, a controlled microporosity is needed. It allows the diffusion of the biopolymer degradation products out of the implant[2] but also controls, over days, months or years,[3] the slow, local and continuous release of loaded drug on the targeted site.[4] In case of biological tissues, especially bone ingrowths, the porosity must be larger (macroporosity) in order to host the cellular and extracellular components of bone and blood vessels.[5] Moreover, most studies suggest that cells have to be interconnected, the interconnections being pathways between cells that favor cellular and vascular penetration and ensure bone ingrowths inside cells. Because interconnections act only as pathways, pore size has to be larger than interconnection size.[6]

Starch is widely used as pharmaceutical material due to its low cost, high availability and non-toxicity. Starch is a semi-crystalline complex polysaccharide mainly composed of linear amylose and non-linear amylopectine. The starch matrix has already shown its potential for biomedical applications.[7–13] Recently, porous plasticized starch was prepared by mixing,[14] microware processing,[15] solvent-exchange process,[16] and by using supercritical CO_2.[17] However, melt-extrusion is a continuous, more productive, easy, and economic process and has been widely used to produce starch-based foams for packaging applications, especially as component in manufacturing loose-fill packaging material.[18–23] Processing temperature, shear rate, humidity, residence time, and cooling temperature are key parameters of the starch foaming by melt-extrusion.[21]

Melt-extrusion of porous materials involves different steps.[24] First, a molten uniform mixture of polymer and gas is formed. The gas can be obtained by different blowing agents (chemical or physical). For starch-based porous materials for biomedical application, water, which is a natural blowing agent, is preferred. The cell germination occurs caused by various sources such as heat, vacuum, the movement, the chemical reaction and cavitation. Germination takes place in a gas-polymer system following a mechanism of homogenous or heterogenous nucleation. The homogenous nucleation (pure medium) occurs when gas molecules dissolve in the homogenous medium (polymer) and when the polymer–gas system is in contact long enough to achieve stable germ of cells. However in practice, solid impurities are often present within the liquid, which play an effective role as a catalyst substrate for nucleation and for reduction of

the interfacial energy. After germination, the cell growth occurs. The key parameters controlling the cell expansion rate are the diffusivity of the gas through the polymer, the gas concentration (a high concentration increases the expansion rate), the viscosity of the mixture (a high viscosity reduces the expansion rate). Finally, the stabilization of the cellular structure takes place, mainly controlled by the cooling rate.

Different authors investigated the physical, mechanical and thermal properties of extruded starch foams.[25–30] Bhatnagar and Hanna[25] extruded high density foams of 25% amylose corn starch with polystyrene and polymethyl methacrylate using bicarbonate and urea as blowing agent and siloxane as cross-linking agents. The effects of temperature and moisture content on the mechanical and rheological properties of starch-based foams containing wheat and corn starches, polyethylene–co-vinyl alcohol and polystyrene with plasticizers and nucleating agents has also been reported.[26] Nabar et al.[27] developed by extrusion hydroxypropylated high-amylose corn starch foam products suitable for cushioning and insulation applications. The cell structure of the foam, which governs the radial expansion, bulk density and other physical properties, was affected by the raw material formulations as well as the extrusion conditions. Heartwin et al.[28] highlighted the influence of talc and polycarbonate on the radial expansion and other physical properties of starch foams. Usage of other fillers such as sugarcane bagasse fibers on the microstructure, density, expansion index, color, water adsorption, and the mechanical properties of extruded starch foams was also studied.[29] Glenn et al.[30] used the heat expansion process to produce starch-based foams using sorbitol, glycerol, ethylene-vinyl alcohol (EVAL), and water. The bulk density was negatively correlated to sorbitol, glycerol, and water content. Increasing the EVAL content increased the bulk density and the observed bulk density was lowest in samples made of wheat and potato starch as compared to corn starch. However, these authors did not characterize the mechanical properties of the materials. The same authors further reported the melt processing of starch-based foam composites with different sources of cellulose fiber using potato starch, glycerol, sorbitol, $CaCO_3$, Mg-stearate and ethylene-vinyl alcohol copolymer. The source of the fiber had little effect on foam density but increased tensile strength and modulus. However, there was no consistent difference in density or tensile properties of samples containing different sources of fiber.[31]

Recent researches have been oriented towards the development of new class of biomaterials, in which inorganic or organo-clay nanoparticles are dispersed in a polymer matrix. These bionanocomposites have shown some interesting advantages compared to neat polymers, as nanofillers addition can improve the mechanical properties but also the control of the release rate of the bioactive agents. Halloysite, aluminosilicate chemically similar to kaolin,[32] can be used as such clay-nanoparticles. Common halloysites used for polymer-based nanocomposites are in form of fine, tubular structures of 300–1500 nm length, 15–100 nm inner diameter, and 40–120 nm outer diameter.[33] Their addition in thermoplastic matrices allows enhancing the mechanical properties,[34–41] thermal properties,[36,37] fire performance,[38] and the degree of crystallinity.[35,37,39] Moreover, their tubular structure is an added advantage for drug delivery systems because they can entrap and then release active ingredient.[42]

Starch is a promising scaffold material for various applications in tissue engineering. Nevertheless, the drawback of a starch scaffold lies in the mechanical weakness, which limits its practical application in tissue engineering.[43–45] The improvement of the mechanical properties of starch scaffolds has been achieved by reinforcing the material with nano-hydroxyapatite (HA)[46] and bioactive glasses.[45] However, these fillers require to be synthesized and need pre-treatment before being used as filler in starch matrix, which limits again their practical applications in tissue engineering. Therefore, using naturally available, cheap, high strength, and biocompatible halloysite nanotubes as fillers appears to be an promising alternative route for the preparation of starch-based scaffolds materials. To our better knowledge, studies on extruded nanocomposite foams based on halloysite nanotubes and starch foams have not been reported yet, even though the combination of these materials may offer various combined advantages such as biocompability, compostability, and improved thermal and mechanical properties.

In that context, the research reported herein focuses on the extrusion of starch foams with halloysite nanotubes by direct melt-blending for biomedical applications such as scaffolds or delivery systems. The suitability of the porous material developed for this purpose depends primarily on the cell size and mechanical properties.[47] In this sense, the effects of moisture, die temperature, and nanotubes content on expansion ratio, cell size, porosity, water uptake, morphological and mechanical properties of nanocomposite foams are some of the key properties that were assessed in this study.

EXPERIMENTAL

Materials

Wheat starch (Roquette, France) was used in this study. In order to limit fluctuation of humidity in starch, it was stored at 23°C with 50% relative humidity (RH). In these conditions, the native starch contains 12% of water (original moisture). The lubricant was glycerol monostearate (Mosselman, Belgium). The plasticizers were glycerol (99% purity) (Sigma–Aldrich, France) and sorbitol (ACROS organics, Belgium). The fillers were as received halloysite nanotubes (HNT) (Natural Nano Inc., USA) which have a density of 2.5 g/cm^3 and a tubular structure with 100–120 nm outer diameter, 60–80 nm inner diameter, and lengths typically ranging from about 500 nm to over 1.2 μm. Before processing, fillers were dried in an oven at 80°C for 12 h in order to eliminate moisture.

Preparation of Porous Plasticized Starch

Porous plasticized starch was produced in two steps. At first, 75 wt % native starch, 24 wt % plasticizer (glycerol or glycerol/sorbitol blend in a ratio of 1:1), and 1 wt % glycerol monostearate were physically blended in a mechanical mixer (Kenwood KMX50, UK) for 30 min at room temperature and then the blend was kept aside for 3 h. For some formulations, additional water is added just before extrusion to reach a total moisture content of 20 wt %. Then, these mixtures were processed in a co-rotating twin-screw extruder (Haake Rheomex PTW 16 OS,

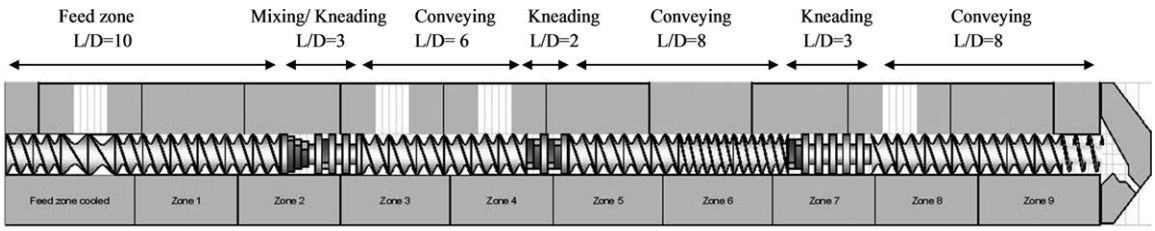

Figure 1. Extrusion screw configuration.

Thermo Scientific, Germany). The screw diameter was 16 mm with *L*/*D* ratio of 40 equipped with a cylindrical die with a diameter of 9 mm. The screw configuration is shown in Figure 1. Screw profile plays an important role in this foaming process; because, plasticization of starch requires thermal energy as well as mechanical energy to form a thermoplastic melt. Hence, the screw configuration had to be so designed to achieve the proper plasticization of granular starch, thus disrupting its crystalline structure and complete dissolution of the blowing agent in the plasticized starch, by promoting convective diffusion under high processing pressure, to form a single phase plastic. The temperature settings from the hopper to intermediates zones were kept constant at 110°C; whereas the die temperature varied from 110 to 145°C. Punctually, the melt temperature was measured with a thermocouple at the die exit. It was the same as the local die temperature set value. This was expected considering the short residence time of the material along the die and the relative low temperature at the die inlet (110°C). It is however worth mentioning that the conclusion regarding temperature values will probably not hold when scaling-up the process, or using a different extruder or die. The screw speed was kept constant at 60 rpm and the feed rate was maintained at 2 kg h^{-1} by a volumetric feeder with 2 min residence time. Plasticized starch was designated as GS for glycerol and GSS for glycerol/sorbitol plasticizer, respectively. To evaluate the influence of halloysite addition, nanocomposites containing 6 wt % HNTs were compounded in the same conditions as the neat porous plasticized starch. This filler loading was decided on the basis of previous works[41] showing that it was an adequate choice to optimize mechanical and thermal properties of thermoplastic starch-based compounds. The resulting compounds were designated as GS6% and GSS6% for HNTs in GS and GSS materials, respectively. The extrudates were air cooled and are cut into samples of approximately 20 mm and were stored in desiccators for four weeks at 23°C or 37°C with a controlled relative humidity (HR) of 53% using saturated solution of magnesium nitrate.

Characterization

The *expansion ratio* (ER) was calculated over 15 samples by dividing the difference between the diameter of the extrudates with and without foaming agent by the internal diameter of the extruder die-nozzle orifice.

The *surface morphology* of the materials was observed by binocular loupe (S-4300SE/N, Hitachi, Japan). Prior to cutting of the foamed samples, they were immersed in resin to secure a sharp incision and avoid crushing of cell walls. The foamed samples were cut in 30 μm slice thick samples with a microtome (Leica RM2165, Switzerland). Particular attention was taken while microtoming of foam samples. Thus, even some edge effects were seen in optical microscopic images (Figure 2), they represent only a very small proportion of the total volume.

The *cell size* of the materials was measured using the image analysis Image J software. Because the cells were not round in shape, the cell size was expressed in area. The average cell size and the cell size distribution were calculated taking into account 10 cuts.

The *porosity* was calculated using the area obtained on ten cuts by the above-mentioned image analysis software according to the following equation.

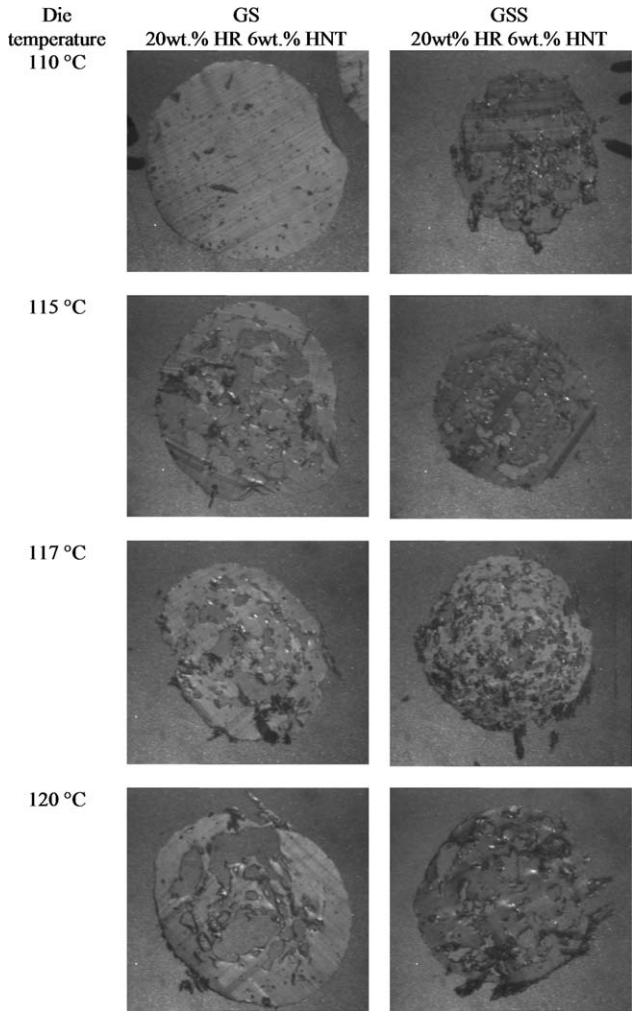

Figure 2. Effect of halloysites content and die temperature on cell size for 6 wt % HNT/starch nanocomposites foams: GS (left) and GSS (right).

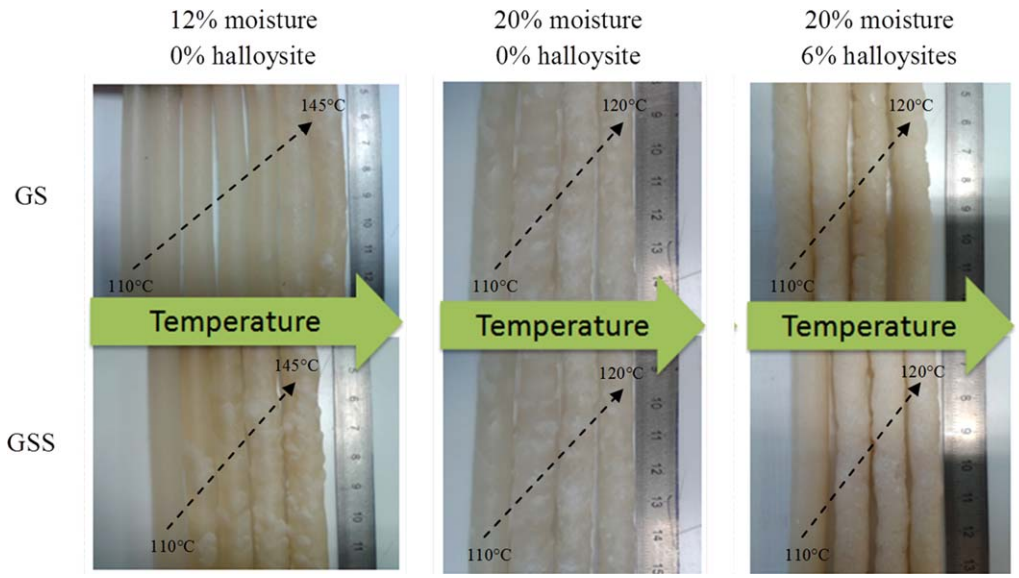

Figure 3. Aspect of extrudates made of neat starch-based foams and 6 wt % HNT/starch nanocomposites foams showing the influence of moisture content, halloysites content and temperature. [Color figure can be viewed in the online issue, which is available at wileyonlinelibrary.com.]

$$\text{Porosity } (\%) = \frac{A_c}{A_t} \times 100 \quad (1)$$

where A_c is the sum of the areas of all cells present on one cut and A_t is the total area of the cut (cell area and matrix area).

Water uptake kinetic was evaluated by immersion of specimens in 20 mL of solution simulating body fluid (pH = 7.4). The specimens were incubated at 37 ± 1°C up to 8 h and, at each time point, samples were blotted with filter paper and accurately weighed. Water uptake, WU (%), was calculated according to the following equation:

$$\text{WU}(\%) = \frac{W_t - W_0}{W_0} \times 100 \quad (2)$$

where W_0 is the dry weight of the foam, and W_t is the wet weight at each time point. Tests were carried out in triplicate.

Mechanical properties in compression were evaluated using cylindrical specimens (diameter $D \approx 10$ mm, height $h = 1.5 * D$) and a tensile machine (Instron, Model 1185) equipped with a 1 kN force sensor at a crosshead speed of 1 mm min^{-1} at 23°C or 37°C. At least five specimens of each composition were tested.

RESULTS AND DISCUSSION

Morphology of Porous Materials

Extrudate Aspect. Figure 3 shows the influence of moisture content, halloysite content, and die temperature on the aspect of the extruded products. With only the natural moisture content (12 wt %), the die temperature must be as high as 140°C or 135°C (for GS or for GSS, respectively) to achieve foaming. These die temperatures are close to the degradation temperature of starch-based materials. However, with additional water content (20 wt % total moisture) starch foam can be obtained at a reduced die temperature of 110°C, albeit with a high heterogenous texture. A die temperature of 117°C is required to achieve a homogenous texture. The extrusion at higher die temperature (>120°C) leads to a dry and brittle product; this is due to the thermal degradation of the compound. The addition of halloysite nanotubes seems to favor the formation homogenous cells in the extrudate.

Expansion Ratio. The expansion of extruded products can be radial or longitudinal expansion. In the present study, only the radial expansion is considered.

The evolution of the expansion ratio as a function of moisture content, halloysite content and die temperature for GS and GSS materials are presented in Figure 4. The effect of die temperature on the expansion ratio involves two opposite phenomena. Firstly, the increase in die temperature leads to an increase in the temperature of polymer/blowing agent mixture, and thus promotes the evaporation of blowing agent (water), accelerates the gas release and therefore can reduce the expansion ratio. Secondly, this same increase in die temperature induces a reduction of the flowing mixture viscosity, a decrease of the rigidity of the cell walls, promotes the cell growth and can favor expansion. For neat materials (GS and GSS), the second phenomenon seems to be predominant and an increase in die temperature leads to an increase in expansion ratio. Conversely, for reinforced materials, the first phenomenon seems to be predominant, because the viscosities are higher, and an increase in the die temperature induces a reduction in the expansion ratio. These results are consistent with those reported by other groups.[48–50]

Surface Morphology. The effect of halloysites and die temperature on cells size for 6 wt % HNT filled GS and GSS nanocomposites is shown in Figure 2. Cells size is not uniform and cells have no particular shape or orientation. The increase of die temperature leads to the evaporation of water inducing an increase of the barrel pressure. After the die exit, water being held at a temperature higher than its boiling point, on exiting the extruder the water within the melt expands due to a sudden

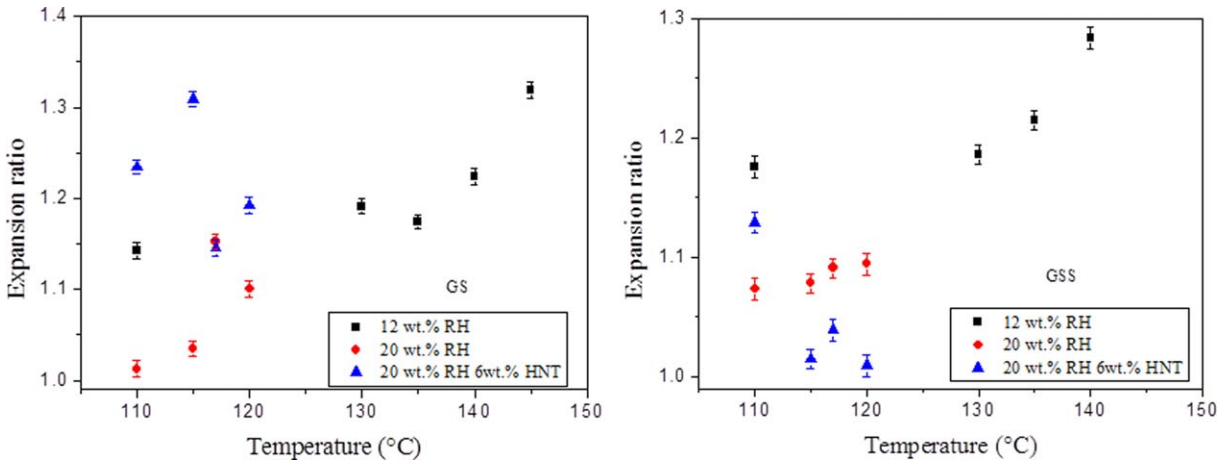

Figure 4. Effect of moisture content, halloysites content and die temperature on expansion ratio for the neat starch-based foams and 6 wt % HNT/starch nanocomposites foams: GS (left) and GSS (right). [Color figure can be viewed in the online issue, which is available at wileyonlinelibrary.com.]

drop in temperature and pressure, thus serving as a blowing agent for the foaming process, this drop in temperature and pressure causes a series of phenomena: initiation of cells, cell growth, and cell coalescence.[51,52]

For all compositions, the increase of the die temperature leads to a refinement of the morphology characterized by an increase of the cell number and by a reduction of the cell size. As previously stated, these observations are the consequence of the viscosity reduction which leads to a higher deformability of the material, which in turn favors the cell growth. However, if the die temperature reaches the degradation temperature (145°C with 12% of moisture content), the material degrades. So, the processing temperature can significantly affect the quality of the foam. Processing at too low die temperature is not favorable to cell growth, and processing at too high die temperature leads to the degradation of material.

Using a high water content (20 wt %) favors the gas generation and the cell formation. By reducing the mixture viscosity (plasticizing effect of water) the cell growth is also promoted. Besides, the presence of halloysite nanotubes leads to a significant increase of the cell number and to a decrease of the cell size. This is due to the fact that, halloysites play the role of nucleating agent and promote initiation of cells. Also, the addition of nanotubes may increase the melt viscosity and induce strain hardening, which could limit cell growth and coalescence.[51]

Porosity. For all materials, the increase in die temperature increases the porosity (Figure 5). The additional water content (20 wt % total moisture) allows attaining the same porosity value (in case of GSS material) or a higher porosity value (in case of GS material) at lower temperature. This phenomenon is due to an increase in the quantity of blowing agent available for foaming, and promotes the formation of cells. Thus, the use of additional water allows decreasing the heat input required to favor the cell nucleation, and thus allows limiting the thermal degradation of the material.[52] The addition of halloysite accentuates these phenomena. The porosity reaches the value of 27.9% at a die temperature equal to 117°C with 20% of moisture content and 6 wt % of halloysite.

Finally, the optimal die temperature (temperature which leads to the higher porosity without thermal degradation of the material) depends on the formulation. At 12% of moisture content, the optimal temperature is equal to 140°C for GS and GSS materials. Further, for 20% of moisture content, with or without halloysite, the optimal die temperature is equal to 117°C for both GS and GSS materials (the optimal porosity and the material non-degradation are achieved).

Pore Size Distribution. The pore size distribution in different foams (neat formulations containing 12 and 20 wt % of water and formulation containing 20 wt % of water and 6 wt % of HNTs), extruded at their optimal die temperature, is presented in Figure 6. The reference material (without additional water content and without halloysite loading) shows a heterogenous distribution of the cell size. Forty percent of the cells are large in size (area > 1 mm^2), 20% of the cells are very small (area < 0.1 mm^2) and the size of the remaining cells is homogeneously distributed between these two extreme limits. The increase in moisture content (20 wt %) leads to an increase in the number of small cells (45% cells which area is inferior 0.1 mm^2) and especially to a reduction of the proportion of large cells (15% cells which area is superior 1 mm^2). This phenomenon is further increased by the presence of halloysite. The half of the cells has a size lower than 0.1 mm^2 which represents a medium diameter of about 350 μm. This cell size is adapted for the biomedical application as scaffold because it permits the formation of cellular and extracellular components of bone and blood vessels.[53]

Properties of Porous Materials

Water Uptake. Figure 7 shows the water uptake of the foamed nanocomposites after an immersion of 8 h at 37°C in the solution simulating body fluid. In the case of foams, the water uptake results from two phenomena: the swelling of the bulk material and the water introduced in the cells. For non-foamed material (the porosity of GS6% extruded at a die temperature at 110°C is very low, 4%, and this material can be considered as

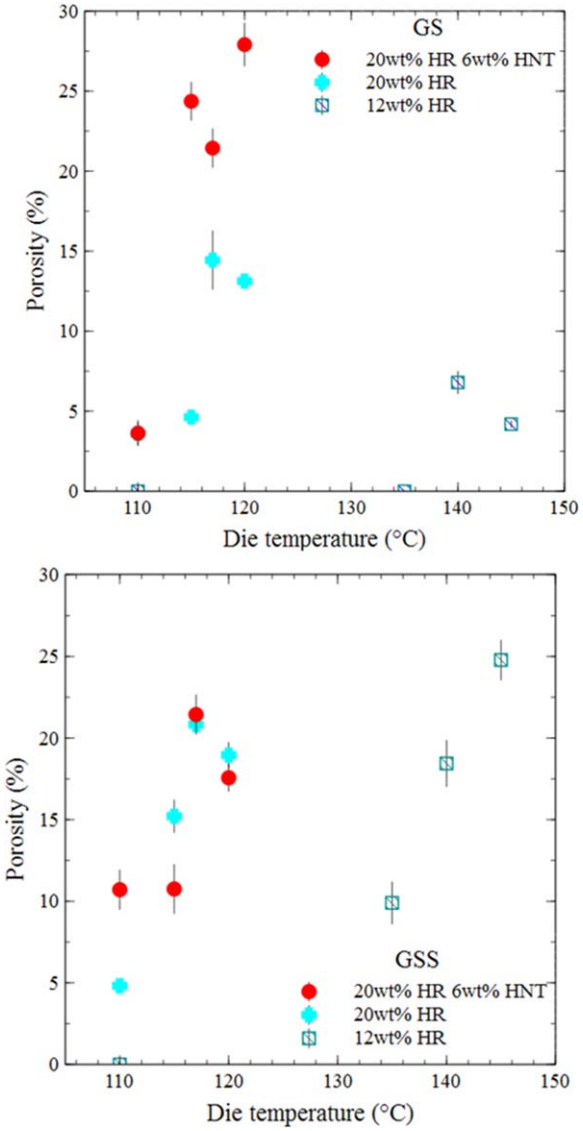

Figure 5. Effect of moisture content, halloysites content and die temperature on porosity for the neat starch-based foams and 6 wt % HNT/starch nanocomposites foams: GS (up) and GSS (down). [Color figure can be viewed in the online issue, which is available at wileyonlinelibrary.com.]

non-foamed), the water content results only from the water absorption during the swelling.[39] Figure 6 shows that the water uptake increases with increasing die temperature. This can be related to the increase of porosity (Figure 4).

Mechanical Behavior in Compression. The porous nanocomposite designated as GSS6% extruded at 117°C die temperature appears to be the best material for scaffold application with 27.9% porosity.[53] Therefore, GSS6% material was selected for the assessment of its mechanical behavior (compression test under multiple loading and unloading). A typical stress–strain curve under uniaxial compression is shown in Figure 8(A) for the porous nanocomposites. This curve can be divided into three parts. At the lower strain values, the starch-based foamed material exhibits a linear elastic behavior. Above a critical strain value, a plateau can be observed. In this zone, cell walls start to

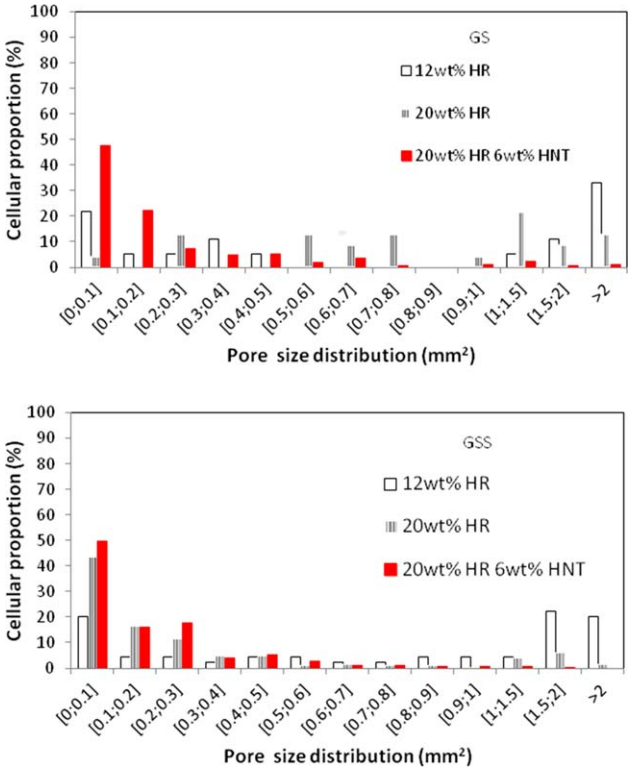

Figure 6. Effect of moisture content and halloysites content on cell size at optimal die temperature for the neat starch-based foams and 6 wt % HNT/starch nanocomposites foams: GS (up) and GSS (down). [Color figure can be viewed in the online issue, which is available at wileyonlinelibrary.com.]

collapse. Finally at a second critical strain value, the cells are completely collapsed, and the stress increases very rapidly for small increments in strain. This zone corresponds to the material densification. The yield point (corresponding to a yield stress of σ_m) characterizes the transition between elastic and plastic behaviors. It can be determined by a tangent method [Figure 8(B)].[54]

For all nanocomposites, the yield stress decreases with increasing die temperature (Figure 9). This can be related to the increase of porosity, which reduces the effective section of the

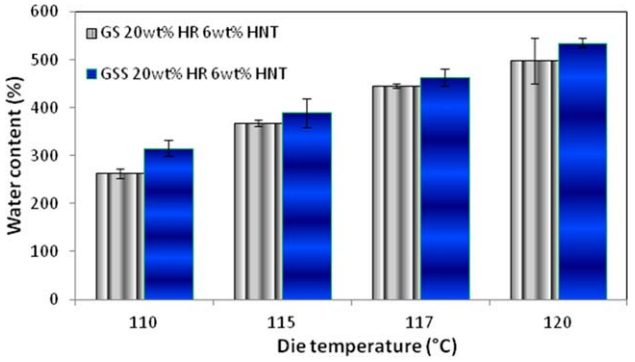

Figure 7. Effect of die temperature on water uptake kinetic for the 6 wt % HNT/starch nanocomposites foams. [Color figure can be viewed in the online issue, which is available at wileyonlinelibrary.com.]

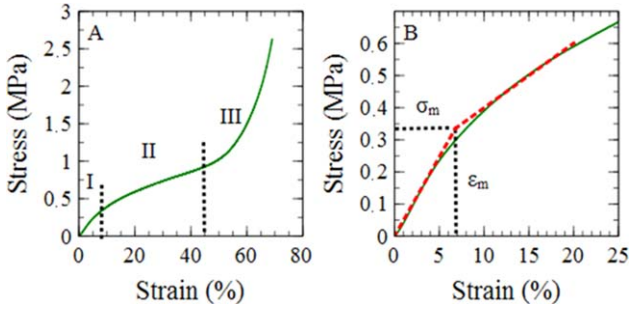

Figure 8. Typical stress–strain curve of the 6 wt % HNT/starch nanocomposites foams under uniaxial compressive loading–unloading (A) and method to obtain yield stress σ_m (B). [Color figure can be viewed in the online issue, which is available at wileyonlinelibrary.com.]

samples. For all the materials, the yield stress increases when the storage temperature increases (Figure 9). The higher chain mobility, coupled with the higher plasticizing effect induced by water uptake, allows delaying the elastic/plastic transition. For further understanding of the compressive properties, yield stress has been plotted as a function of porosity (Figure 10). Mechanical properties of the starch/halloysite nanocomposite foams are largely dependent on the porosity. The highest compressive stress (0.85 MPa) was observed at a porosity of 4%, whereas the lowest compressive stress (0.45 MPa) was observed at a porosity of 28%. Low porous foams tend to have thicker cell walls or higher solid fraction and hence are able to resist deformation

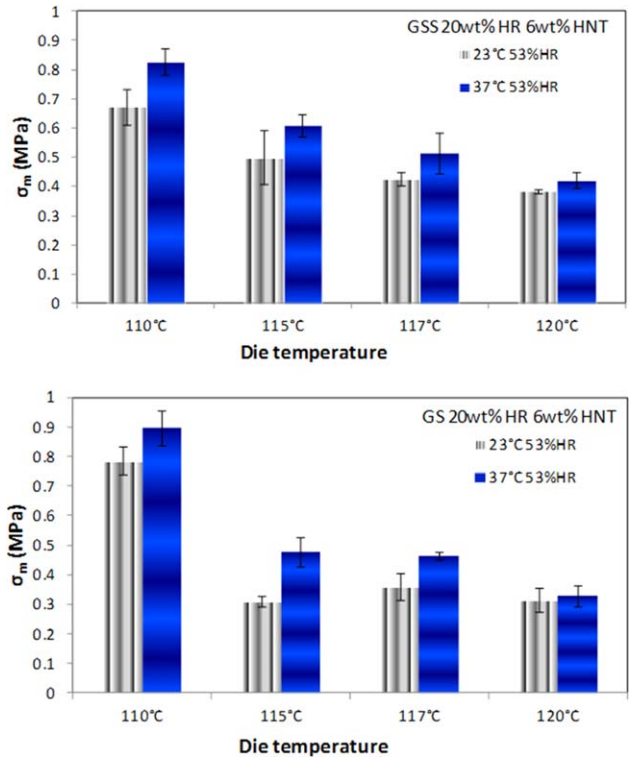

Figure 9. Effect of die temperature and storage parameters (temperature and relative humidity) on yield stress in compression of 6 wt % HNT/starch nanocomposites foams: GS (up) and GSS (down). [Color figure can be viewed in the online issue, which is available at wileyonlinelibrary.com.]

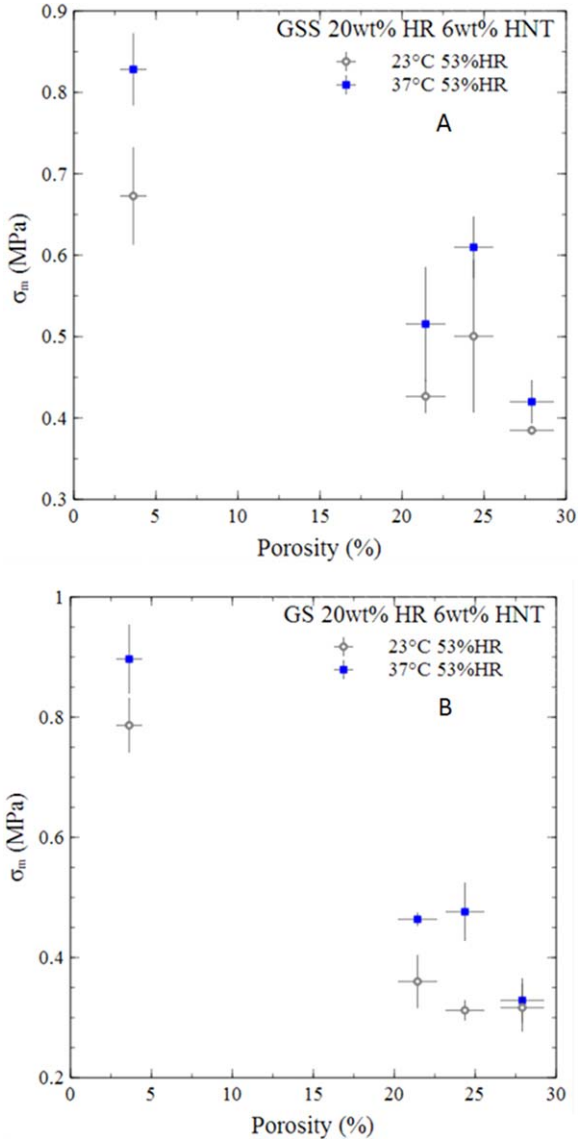

Figure 10. Compressive yield stress as a function of porosity for 6 wt % HNT/plasticized starch nanocomposites foams: GSS (A) and GS (B). [Color figure can be viewed in the online issue, which is available at wileyonlinelibrary.com.]

better than high porous foams with thinner cell walls. The few exceptions in some samples may be attributed to specimen heterogeneity.

CONCLUSIONS

Plasticized starch-based nanocomposites foams were successfully prepared by melt-extrusion using water as a blowing agent. The expansion ratio and the porosity increase with increasing die temperature. Increasing the water content (blowing agent content) allows reducing the minimal die temperature required to achieve the foaming process and limits the risk for material degradation. The addition of halloysite nanotubes in the plasticized starch matrix favors the cell nucleation and decreases the cell size. Halloysite nanotubes act not only as a nucleating agent but

also as a barrier which limits the cell growth leading to macroporosity in material.

Finally, porous nanocomposites based on plasticized starch with a blend of glycerol and sorbitol and containing 6 wt % of halloysite, produced at a die temperature of 117°C, seems to combines several important features (high porosity, macroporosity promoting the formation of cellular and extracellular components of bone and blood vessels and adequate mechanical strength) required for bone substitutes or bone cements applications

ACKNOWLEDGMENTS

The authors are indebted to CISIT (International Campus on Safety and Intermodality in Transportation), the Nord-Pas-de-Calais Region, and European Community (FEDER) for their financial support.

REFERENCES

1. Baker, S.C.; Rohman, G.; Southgate, J.; Cameron, N. R. *Biomaterials* **2009**, *30*, 1321.
2. Gauthier, O.; Bouler, J. M.; Aguado, E.; Pilet, P.; Daculsi, G. *Biomaterials* **1998**, *19*, 133.
3. Chevalier, E.; Chulia, D.; Pouget, C.; Viana M. *J. Pharm. Sci.* **2008**, *97*, 1135.
4. Hasegawa, M.; Sudo, A.; Komlev, V. S.; Barinov, S. M.; Uchida, A. *J. Biomed. Mater. Res. Part B: Appl. Biomater.* **2004**, *70B*, 332.
5. Hulbert, S. F.; Morrison, S. J.; Klawitter, J. J. *J. Biomed. Mater. Res. Symp.* **1971**, *2*, 269.
6. Lu, J. X.; Flautre, B.; Anselme, K.; Hardouin, P.; Gallur, A.; Descamps, M.; Thierry, B. *J. Mater. Sci. Mater. Med.* **1999**, *10*, 111.
7. Henrist, D.; Lefebvre, R.; Remon, J. P. *Int. J. Pharm.* **1999**, *187*, 185.
8. Gomes, M. E.; Godinho, J. S.; Tchalamov, D.; Cunha, A. M.; Reis, R. L. *Mater. Sci. Eng. C: Biomim. Supramol. Syst.* **2001**, *20*, 19.
9. Elvira, C.; Manoa, J. F.; San Román, J.; Reisa, R. L. *Biomaterials* **2002**, *23*, 1955.
10. Salgado, A. J.; Coutinho, O. P.; Reis, R. L.; Davies, J. E. *J. Biomed. Mater. Res. Part A* **2007**, *80A*, 983.
11. Balmayor, E. R.; Tuzlakoglu, K.; Azevedo, H. S.; Reis, R. L. *Acta Biomater.* **2009**, *5*, 1035.
12. Freire, C.; Podczeck, F.; Veiga, F.; Sousa, J. *Eur. J. Pharm. Biopharm.* **2009**, *72*, 587.
13. Saboktakin, M. R.; Tabatabaie, R. M.; Maharramov, A.; Ramazanov, M. A. *Int. J. Biol. Macromol.* **2011**, *48*, 381.
14. Shi, R.; Liu, Q.; Ding, T.; Han, Y.; Zhang, L.; Chen, D.; Tian, W. *J. Appl. Polym. Sci.* **2006**, *103*, 574.
15. Torres, F. G.; Boccaccini, A. R.; Troncoso, O. P. *J. Appl. Polym. Sci.* **2007**, *103*, 1332.
16. Wu, C.; Wang, Z.; Zhi, Z.; Jiang, T.; Zhang, J.; Wang, S. *Int. J. Pharm.* **2011**, *403*, 162.
17. Miao, Z.; Ding, K.; Wu, T.; Liu, Z. M.; Han, B. X.; An, G. M.; Miao, S. D.; Yang, G. Y. *Micropor. Mesopor. Mater.* **2008**, *111*, 104.
18. Li, H. B.; Huneault, M. A. *J. Appl. Polym. Sci.* **2011**, *122*, 134.
19. Nabar, Y.; Narayan, R. *J. Appl. Polym. Sci.* **2006**, *101*, 3983.
20. Zhou, J.; Hanna, M. A. *Starch-Starke* **2004**, *56*, 484.
21. Aguilar-Palazuelos, E.; Zazueta-Morales, J. D. J.; Jiménez-Arévalo, O. A.; Martínez-Bustos, F. *Starch-Stärke* **2007**, *59*, 533.
22. Pushpadass, H. A.; Babu, G. S.; Weber, W. R.; Hanna, M. A. *Packag. Technol. Sci.* **2008**, *21*, 171.
23. Benezet, J. C.; Stanojlovic-Davidovic, A.; Bergeret, A.; Ferry, L.; Crespy, A. *Ind. Crop. Prod.* **2012**, *37*, 435.
24. Babin, P.; Dellavalle, G.; Dendievel, R.; Lourdin, D.; Salvo, L. *Carbohyd. Polym.* **2007**, *68*, 329.
25. Bhatnagar, S.; Hanna, M. A. *Cereal Chem.* **1996**, *73*, 601.
26. Cha, J.; Chung, D. S.; Seib, P. A. *Trans. ASAE* **1999**; *42*, 1765.
27. Nabar, Y.; Narayan, R.; Schindler, M. *Polym. Eng. Sci.* **2006**, *46*, 438.
28. Heartwin, A. P.; Govindarajan, S. B.; Robert, W. W.; Hanna, A. M. *Packag. Technol. Sci.* **2008**, *21*, 171.
29. Malia, S.; Debiagia. F.; Maria, V. E. G.; Yamashitab, F. *Ind. Crops Prod.* **2010**, *32*, 353.
30. Glenn, G. M.; Klamczynski, A.; Holtman, K. M.; Chiou, B. S.; Orts, W. J.; Wood, D. *J. Biobased Mater. Bioenerg.* **2007**, *1*, 360.
31. Glenn, G. M.; Klamczynski, A. K.; Holtman, K. M.; Shey, J.; Chiou, B. S.; Berrios, J.; Wood, D.; Orts, W. J.; Imam, S. H. *J. Agric. Food Chem.* **2007**, *55*, 3936.
32. Joussein, E.; Petit, S.; Chruchman, J.; Theng, B.; Righi, D.; Delvaux, B. *Clay Mineral* **2005**, *40*, 383.
33. Du, M.; Guo, B.; Jia, D. *Polym. Int.* **2010**, *59*, 574.
34. Prashantha, K.; Lacrampe, M.-F.; Krawczak, P. *Express Polym. Lett.* **2011**, *5*, 295.
35. Prashantha, K.; Schmitt, H.; Lacrampe, M.-F.; Krawczak, P. *Compos. Sci. Technol.* **2011**, *71*, 1859.
36. Ismail, H.; Pasbakhsh, P.; Fauzi, M. N. A.; Abu Bakar, A. *Polym. Test.* **2008**, 841.
37. Xie, Y.; Chang, Y.; Wang, S.; Yu, J.; Ma, X. *Carbohyd. Polym.* **2011**, *83*, 186.
38. Marney, D. C. O.; Ruisell, L.; Wu, D. Y. *Polym. Degrad. Stab.* **2008**, *93*, 1971.
39. Szczygielska, A.; Kijeński, J. *Polish J. Chem. Technol.* **2011**, *13*, 61.
40. Schmitt, H.; Prashantha, K.; Soulestin, J.; Lacrampe, M. F.; Krawczak, P.; Raquez J. M. *Adv. Mater. Res.* **2012**, *584*, 445.
41. Schmitt, H.; Prashantha, K.; Soulestin, J.; Lacrampe, M. F.; Krawczak, P. *Carbohydr. Polym.* **2012**, *89*, 920.
42. Schmitt, H.; Creton, N.; Prashantha, K.; Soulestin, J., Lacrampe, M. F.; Krawczak, P. *Polym. Eng. Sci.* **2014**, 10.1002/per.23919.

43. Gomes, M. E.; Ribeiro, A. S.; Malafaya, P. B.; Reis, R. L.; Cunha, A. M. *Biomaterials* **2001**, *22*, 883.

44. Gomes, M. E.; Godinho, J.; Tchalamov, D.; Cunha, A.; Reis, R. *J. Appl. Med. Polym.* **2002**, *6*, 75.

45. Leonor, I. B.; Sousa, R. A.; Cunha, A. M.; Reis, R. L.; Zhong, Z. P.; Greenspan, D. **2002**, *J. Mater. Sci. Mater. M 13*, 939.

46. Sundaram, J.; Durance, T. D.; Wang, R. *Acta Biomater.* **2008**, *4*, 932.

47. Goswami, J.; Bhatnagar, N.; Mohanty, S.; Ghosh, A. K. *Express Polym. Lett.* **2013**, *7*, 767.

48. Park, C. B.; Behravesh, A. H.; Venter, R. D. *Polym. Eng. Sci.* **1998**, *38*, 1812.

49. Klempner, D.; Sendijarevic, V., Handbook of Polymeric Foams and Foam Technology, 2nd d.; Hanser Gardner Publications: Munich, **2004**, p 154.

50. Julien, J.-M.; Bénézet, J.-C.; Lafranche, E.; Quantin, J.-C.; Bergeret, A.; Lacrampe, M.-F.; Krawczak, P. *Polymer* **2012**, *53*, 5885.

51. Lee, L. J.; Zheng, C.; Cao, X.; Han, X.; Shen, J.; Xu, G. *Compos. Sci. Technol.* **2005**, *65*, 2344.

52. Wu, W.; Cao. X.; Zhang, Y. J.; He, G. J. *J. Appl. Polym. Sci.* **2013**, *130*, 443.

53. Tai, H.; Mather, M. L.; Howard, D.; Wang, W.; White, L. J.; Crowe, J. A.; Morgan, S. P.; Chandra, A.; Williams, D. J.; Howdle, S. M.; Shakesheff, K. M. *Eur. Cells Mater.* **2007**, *14*, 64.

54. Viot, P. *Int. J. Impact Eng.* **2009**, *36*, 945.